The recognition of anions using delayed lanthanide luminescence: The use of Tb(III) based urea functionalised cyclen complexes

Cidália M. G. dos Santos and Thorfinnur Gunnlaugsson

Electronic Supporting Information

Figure S1 ^{1}H-NMR (400 MHz, $CDCl_3$) of ligand **1**

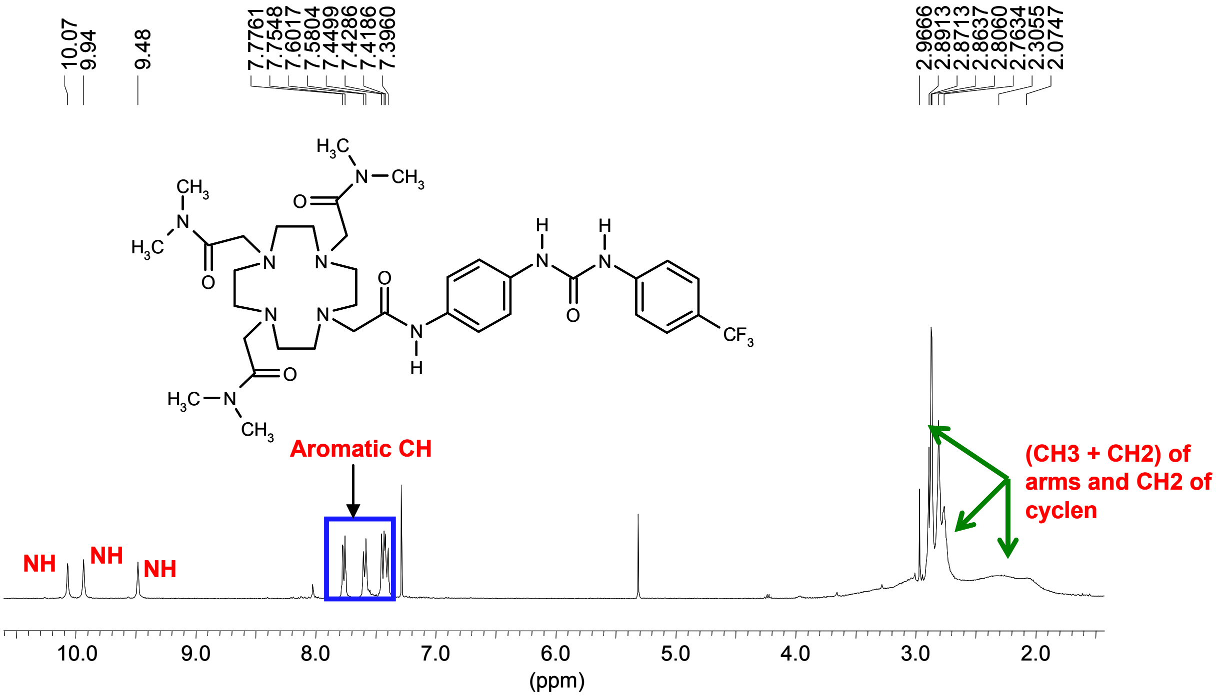

Figure S2a ^{1}H-NMR (400 MHz, CD_3OD) of **Tb.1**

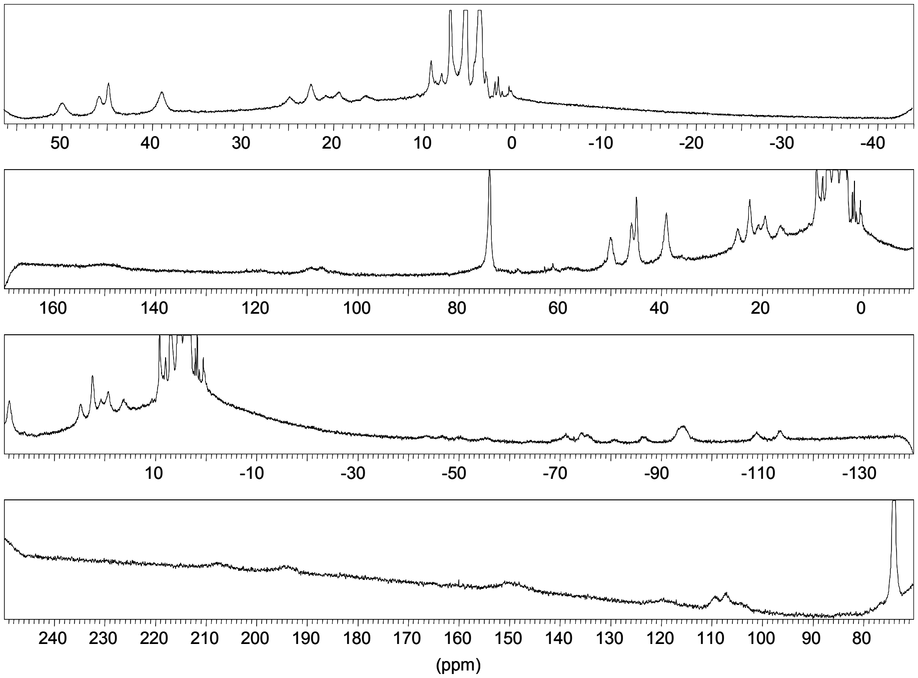

Figure S2b ESMS of **Tb.1** showing the Tb(III) characteristic isotopic distribution pattern for the M/2 peak

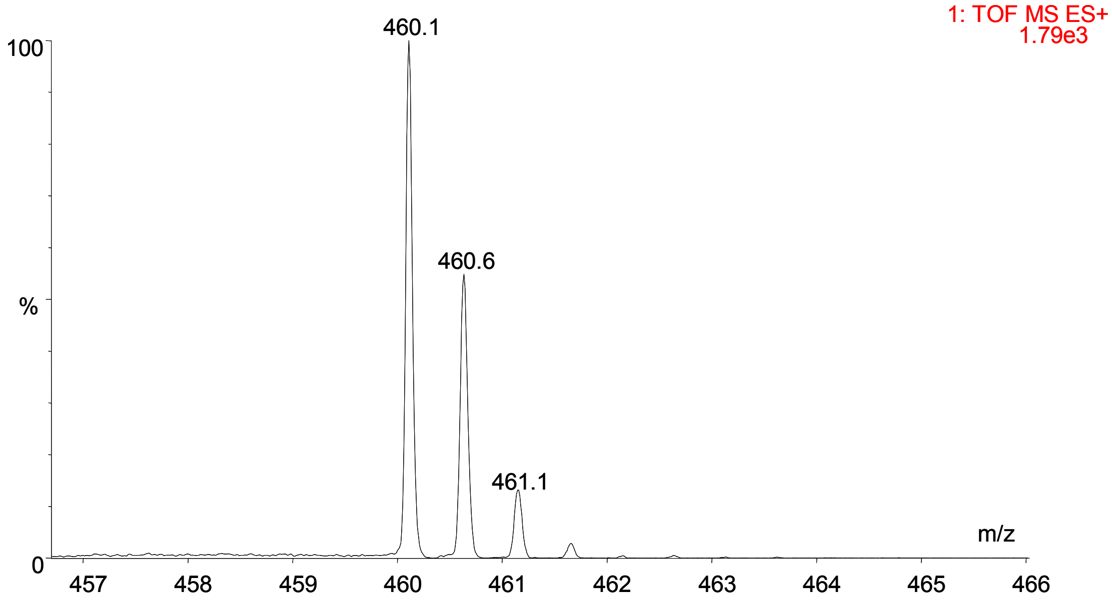

Figure S2c ESMS of **Eu.1** showing the Eu(III) characteristic isotopic distribution pattern for the [M + CF_3SO_3]/2 peak

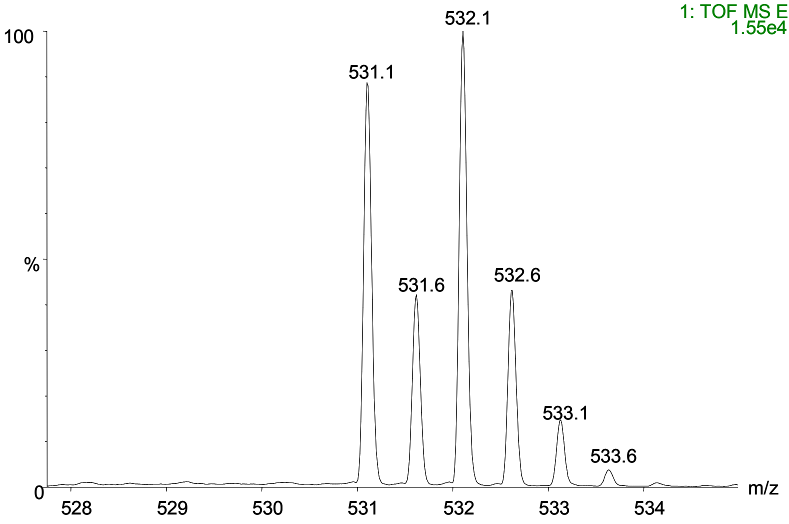

Figure S3 Changes in the absorption spectra of **Tb.1** (4µM) upon gradual additions of $H_2P_2O_7^{2-}$ (0 → 56.3 µM) in CH_3CN. Insert shows the titration profile for the changes at 270 nm versus the equivalents of $H_2P_2O_7^{2-}$.

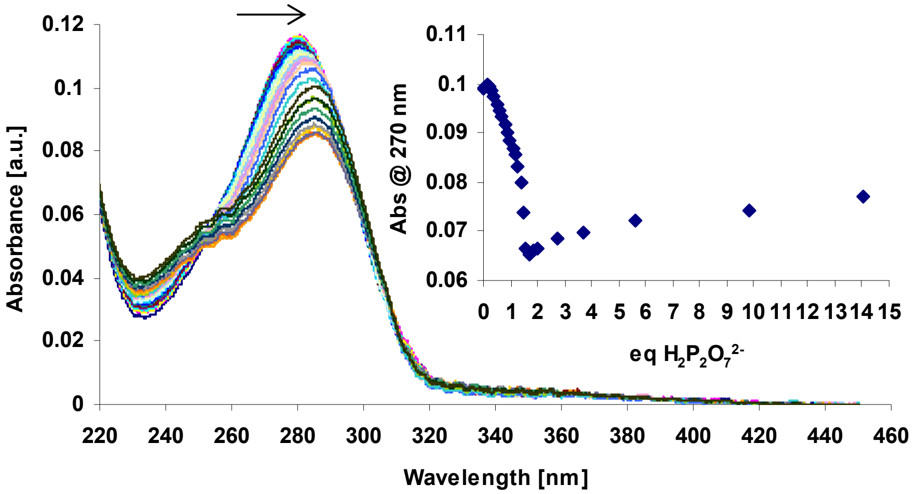

Figure S4 Speciation distribution diagram obtained for the absorption titration of **Tb.1** (H) with $H_2P_2O_7^{2-}$ (G). Insert: The experimental binding isotherm and corresponding fit obtained using SPECFIT.

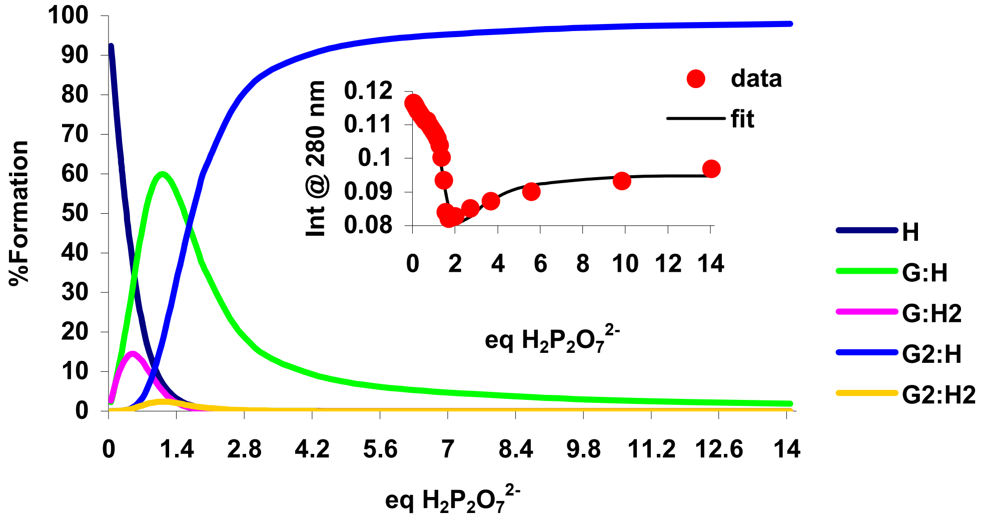

Figure S5 Experimental binding isotherm for the absorption titration of **Tb.1** (4μM) with $H_2PO_4^-$ and corresponding fit obtained using SPECFIT.

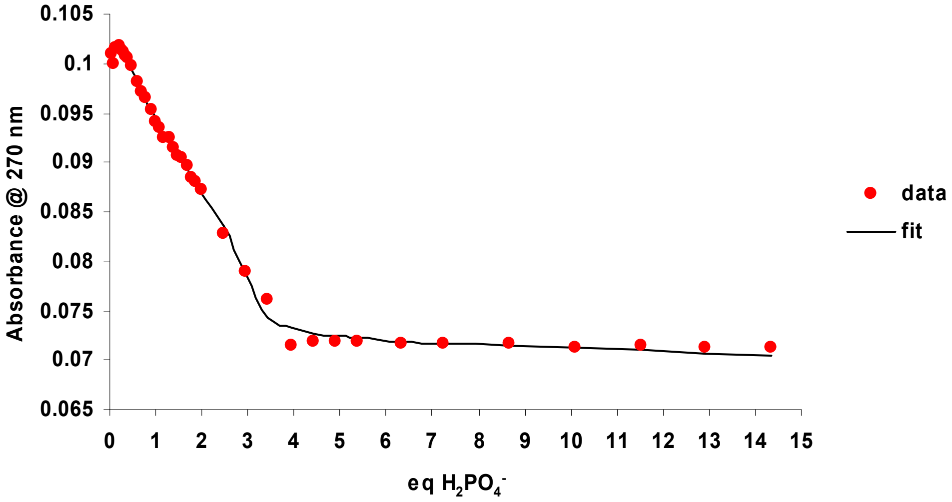

Figure S6 Absorption spectra showing the changes in the absorbance of **Tb.1** (4μM) upon gradual additions of: **a)** 0 → 7 equivalents of F^-; **b)** 8 → 17 equivalents of F^-, light blue line represents free **Tb.1**

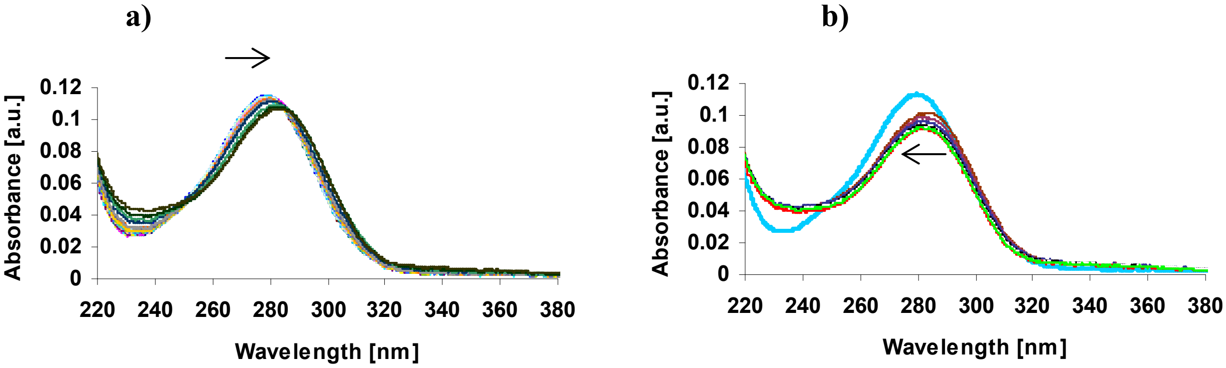

Figure S7 Speciation distribution diagram obtained for the absorption titration of **Tb.1** (H) with F^- (G).

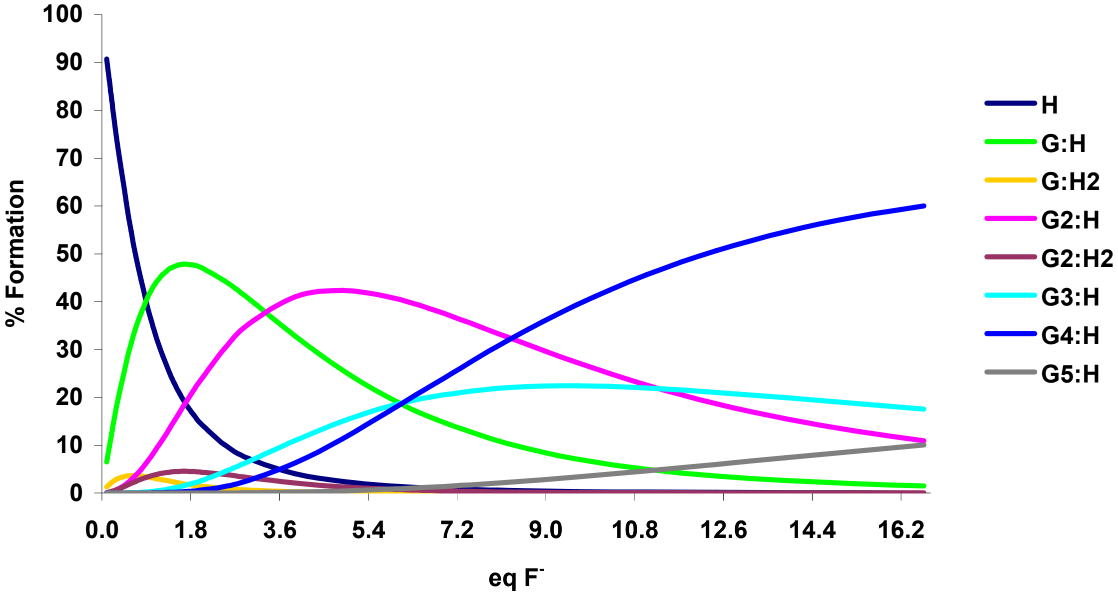

Figure S8 Absorption spectra showing the changes in the absorbance of **Tb.1** (4μM) upon gradual additions of Cl^- (0 → 28.1 μM) in CH_3CN. Insert: The titration profile for the changes at 264 nm versus the equivalents of Cl^-

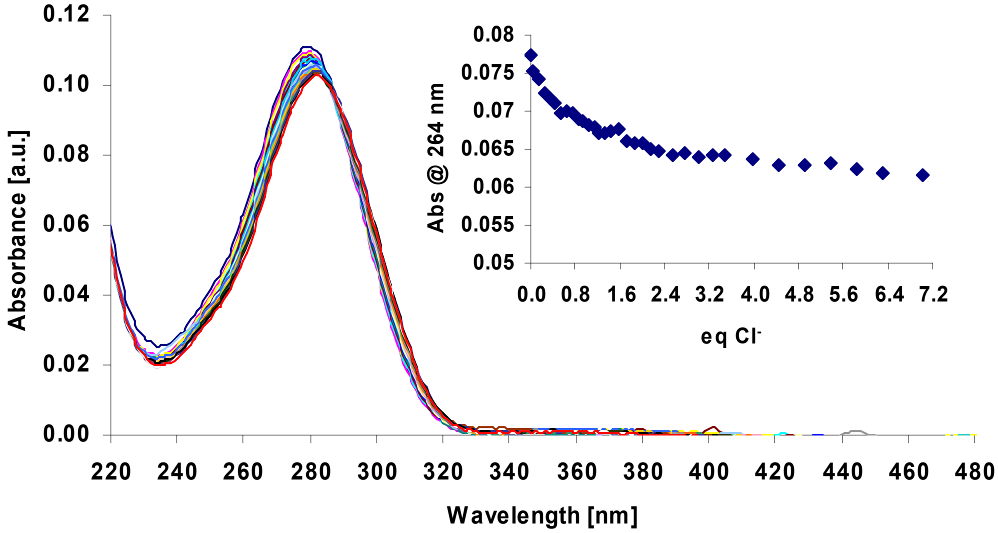

Figure S9 Changes in the fluorescence spectra of **Tb.1** (4μM) upon gradual additions of $H_2PO_4^-$ (0 → 57.3 μM) in CH_3CN. Insert: The titration profile for the changes at 422 nm versus the equivalents of $H_2PO_4^-$

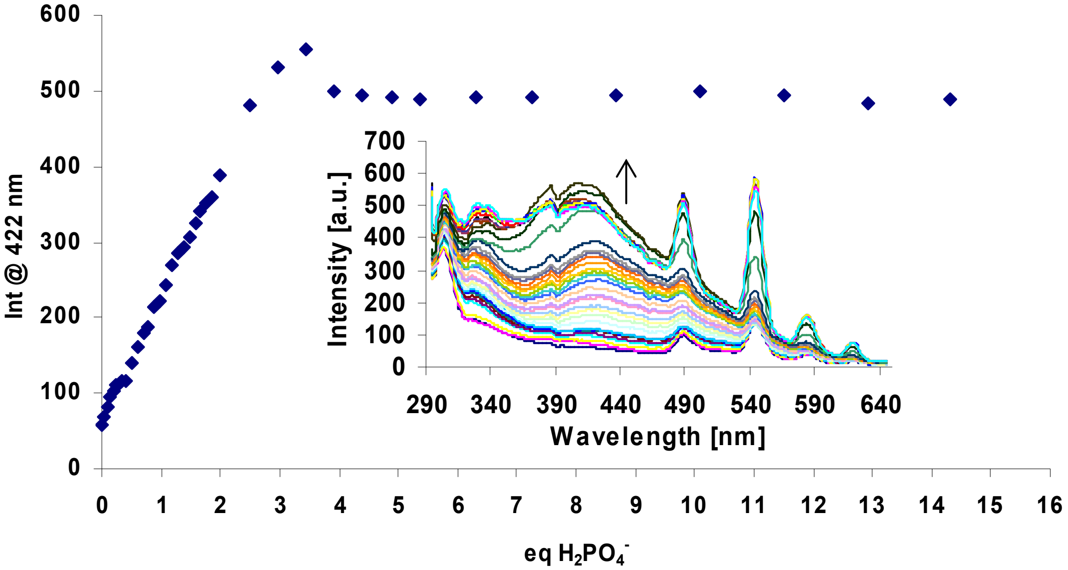

Figure S10 a) Changes in the fluorescence spectra of **Tb.1** (4μM) upon gradual additions of F^- (0 → 56.3 μM) in CH_3CN. Insert: Changes observed between 0 → 5 equivalents of F^-; **b)** Titration profile for the changes at 334 and 422 nm, versus the equivalents of F^-

a)

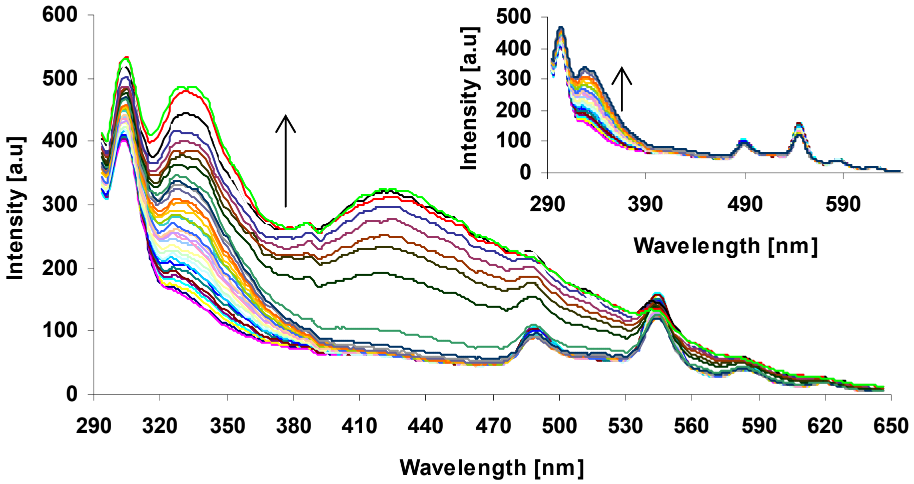

b)

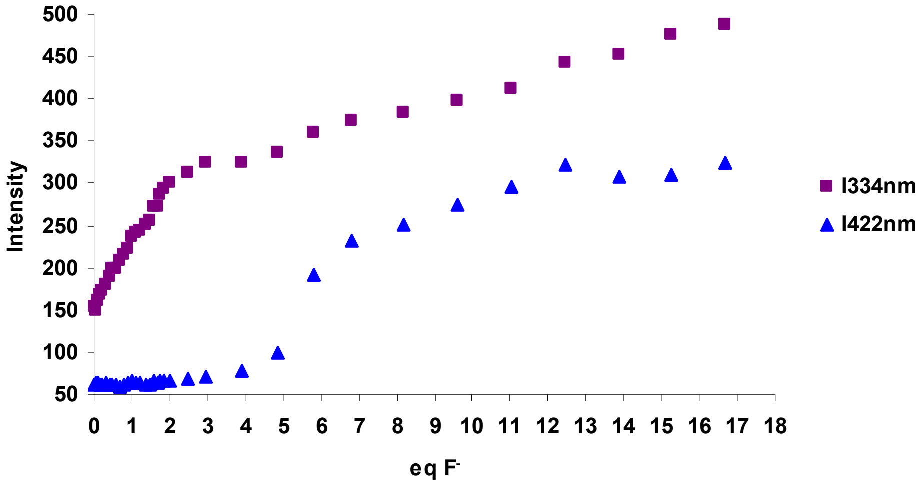

Figure S11 Changes in the fluorescence spectra of **Tb.1** (4μM) upon gradual additions of Cl^- (0 → 28.1 μM) in CH_3CN. Insert: The titration profile for the changes at 330 nm versus the equivalents of Cl^-

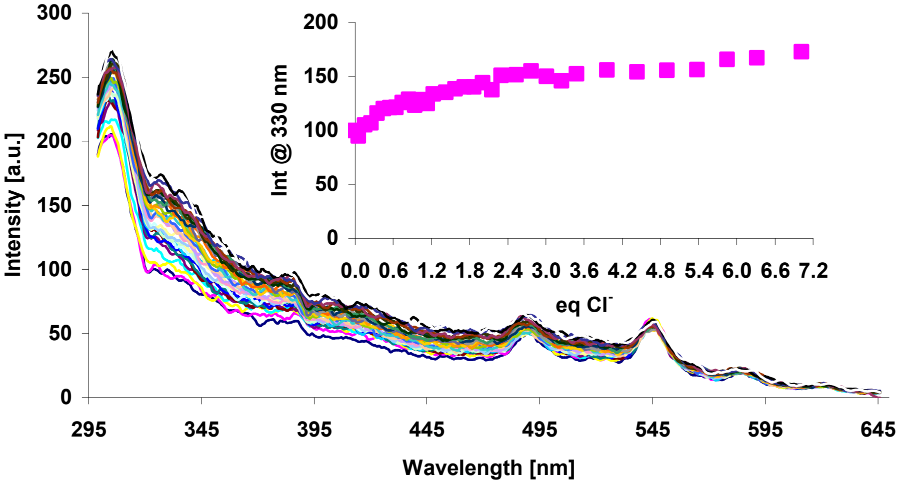

Figure S12 Changes in the lanthanide emission intensity of **Tb.1** (4μM) upon gradual additions of CH_3COO^- (0 → 74.9 μM) in CH_3CN

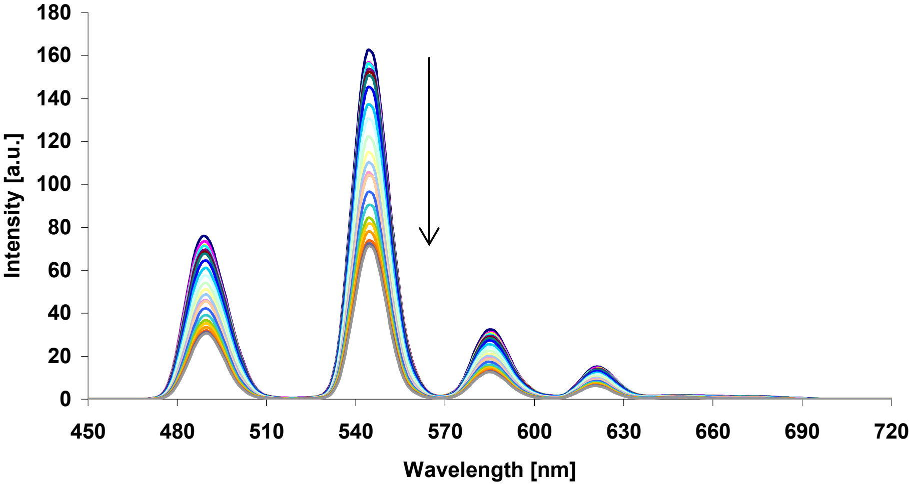

Figure S13 Experimental binding isotherm for the lanthanide luminescence titration of **Tb.1** (4μM) with CH_3COO^- and corresponding fit obtained using SPECFIT

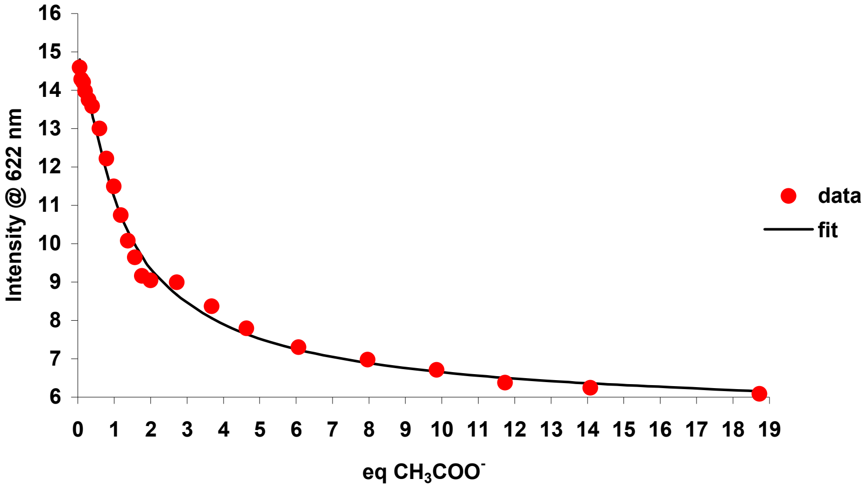

Figure S14 The changes in the lifetimes of the **Tb.1** emission upon titration with $H_2PO_4^-$. These results mirror the changes in the Tb(III) emission intensity shown in Figure 10 in the manuscript

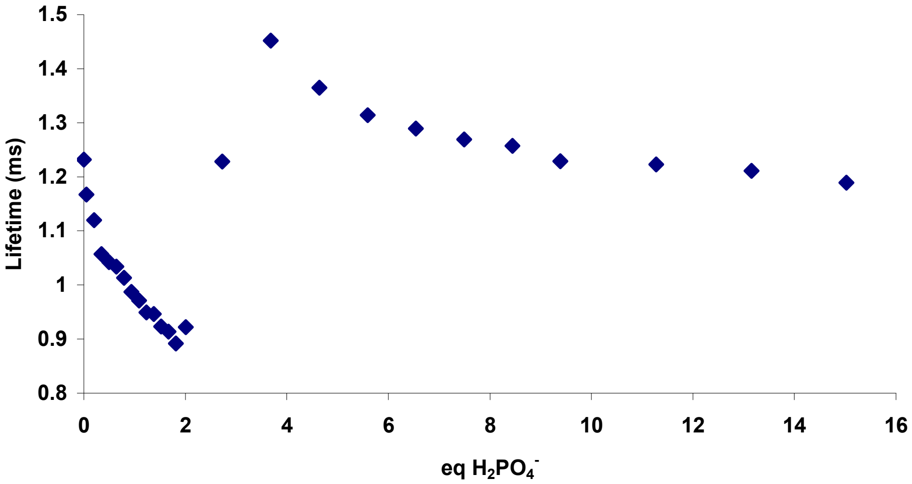

Figure S15 Profile of the Tb(III) emission intensity at 546 nm versus the equivalents of $H_2P_2O_7^{2-}$. Insert: The family of spectra obtained upon titration of **Tb.1** (4μM) with $H_2P_2O_7^{2-}$ (0 → 56.3 μM) in CH_3CN

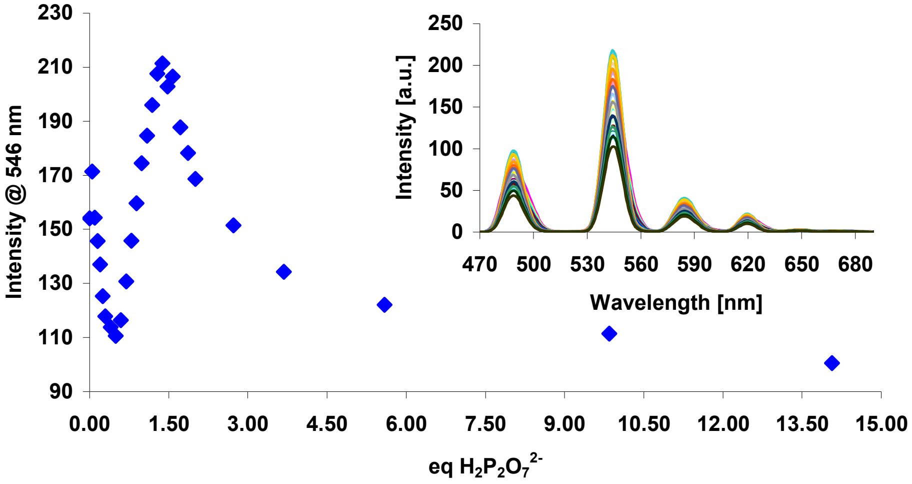

Figure S16 Speciation distribution diagram for the lanthanide luminescence titration of **Tb.1** (H) with $H_2P_2O_7^{2-}$ (G). Insert: The experimental binding isotherm and corresponding fit using SPECFIT

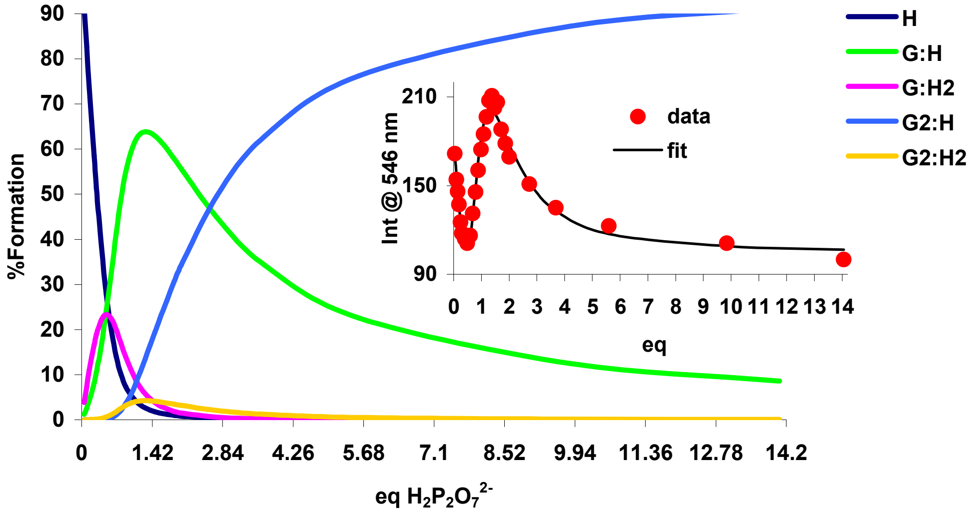

Figure S17 The Tb(III) luminescence spectra of **Tb.1** (H) upon gradual additions of F^- (0 → 66.6 μM) in CH_3CN. Insert: The changes at 546 nm versus the equivalents of F^-

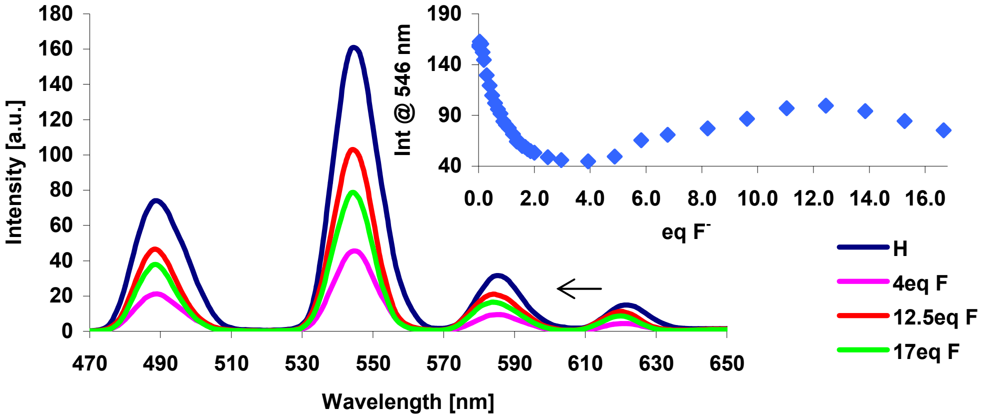

Figure S18 Changes in the lanthanide emission of **Tb.1** (4μM) upon gradual additions of Cl^- (0 → 28.1 μM) in CH_3CN. Insert: The changes at 546 nm versus the equivalents of Cl^-

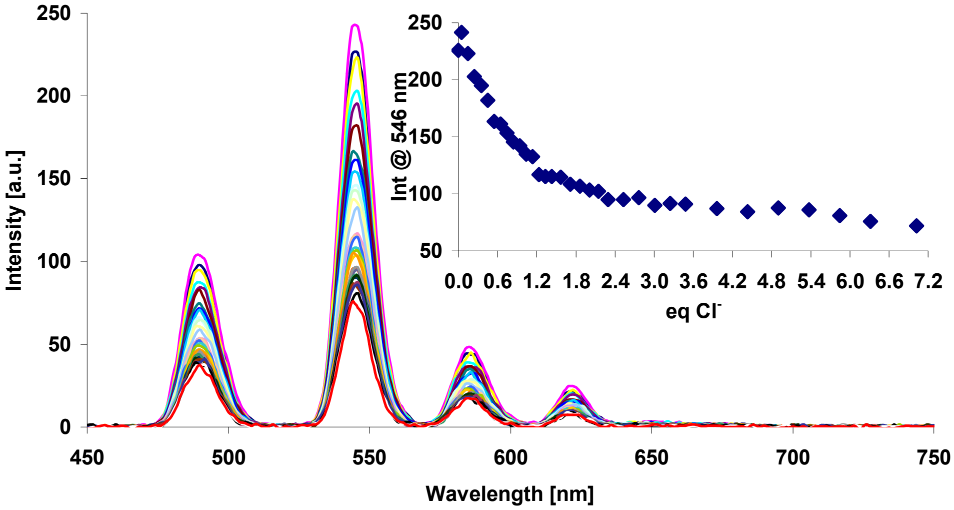

Figure S19 Speciation distribution diagram for the lanthanide luminescence titration of **Tb.1** (H) with Cl$^-$ (G). Insert: The experimental binding isotherm and corresponding fit using SPECFIT